Received: 10 February 2018 | Revised: 3 July 2018 | Accepted: 5 July 2018

DOI: 10.1002/pip.3068

RESEARCH ARTICLE

WILEY PROGRESS IN PHOTOVOLTAICS

Tabula Rasa for *n*-Cz silicon-based photovoltaics

Vincenzo LaSalvia[1] | Amanda Youssef[2] | Mallory A. Jensen[2] | Erin E. Looney[2] | William Nemeth[1] | Matthew Page[1] | Wooseok Nam[3] | Tonio Buonassisi[2] | Paul Stradins[1]

[1] National Renewable Energy Laboratory, Golden, CO, USA

[2] Massachusetts Institute of Technology, Cambridge, MA, USA

[3] Woongjin Energy Co. Ltd., Daejoen, Korea

Correspondence
Vincenzo LaSalvia, National Renewable Energy Laboratory, National Center for Photovoltaics, Golden, CO, USA.
Email: vincenzo.lasalvia@nrel.gov

Funding information
US Department of Energy (Office of Energy Efficiency and Renewable Energy; Solar Energy Technology Office, Grant/Award Numbers: DE-AC36-08GO28308, DEEE00030301; National Science Foundation, Grant/Award Number: 1122374

Abstract

High-temperature annealing, known as *Tabula Rasa* (TR), proves to be an effective method for dissolving oxygen precipitate nuclei in *n*-Cz silicon and makes this material resistant to temperature-induced and process-induced lifetime degradation. *Tabula Rasa* is especially effective in *n*-Cz wafers with oxygen concentration >15 ppma. Vacancies, self-interstitials, and their aggregates result from TR as a metastable side effect. Temperature-dependent lifetime spectroscopy reveals that these metastable defects have shallow energy levels ~0.12 eV. Their concentrations strongly depend on the ambient gases during TR because of an offset of the thermal equilibrium between vacancies and self-interstitials. However, these metastable defects anneal out at typical cell processing temperatures ≥850°C and have little effect on the bulk lifetime of the processed cell structures. Without dissolving built-in oxygen precipitate nuclei, high-temperature solar cell processing severely degrades the minority carrier lifetimes to below 0.1 millisecond, while TR-treated *n*-Cz wafers after the cell processing steps exhibit carrier lifetimes above 2.2 milliseconds.

KEYWORDS

bulk lifetime, diffused boron emitter, intrinsic point defects, *n*-type Czochralski, oxygen precipitation, photovoltaics, *Tabula Rasa*, thermally induced degradation

1 | INTRODUCTION

In this work, we identify the physical mechanisms behind the thermally induced degradation (TID) throughout the solar cell process using *n*-Cz Si wafers. In contrast with *p*-type Cz wafers common to the mainstream PV industry, *n*-Cz wafers do not exhibit light-induced degradation (LID), and are considerably more resistant to recombination introduced by transition metal impurities. Yet, boron diffusion, used to create the p-n junction for *n*-Cz wafers, requires higher process temperatures and longer times than its phosphorus diffusion analog process in *p*-Cz wafers. Bulk carrier lifetimes degrade strongly during the high-thermal budget part of the boron emitter formation, namely a deep drive-in performed typically near 980°C.[1] If the TID is mitigated in *n*-Cz Si, one could anticipate reaching cell efficiencies above 24%, as record efficiencies in cells with deep boron emitter on *n*-FZ wafers with high (multiple millisecond) photocarrier lifetime are reported as high as 25.7%.[2]

To mitigate the TID in *n*-Cz, Walter et al[3] proposed short thermal anneals prior to cell processing known as *Tabula Rasa* (TR).[4] Oxygen precipitates, especially decorated with Fe, were identified by Murphy[5] as recombination sources associated with TID in both *n*-type and *p*-type Cz silicon. Recently, Basnet et al have shown that the elimination of oxygen precipitate nuclei through TR along with the removal of impurities through phosphorus gettering can lead to significantly improved bulk lifetimes of upgraded metallurgical grade (UMG) silicon wafers.[6]

In this work, we show that in general the degradation in the bulk minority carrier lifetime in *n*-Cz Si, provided the solar cell processing is sufficiently uncontaminated, is governed by the point defects, both built-in from the Czochralski growth and introduced by or mitigated by thermal process steps. High lifetime *n*-type Cz-Si contains interstitial oxygen [O_i] in excess of 5.0×10^{17} cm^{-3}. During the lengthy cool-down of the *n*-Cz Si ingot, grown-in intrinsic point defects (vacancies and their agglomerates) react with interstitial oxygen to

form oxygen precipitate nuclei (OPN). And, during cell processing above 900°C, they develop into 10 to 100 nm size O precipitates. *Tabula Rasa* annealing before the cell process dissolves all OPN that are below critical size at the temperature of TR (typically above 1000°C). This critical size is larger at higher temperature.[7] This returning to a "clean slate" of the *n*-Cz Si with atomically dispersed interstitial O_i considerably delays repeated nucleation and growth of the OPNs during the cell process at high thermal budget. We observe that this dissolution is accompanied by the formation of other, metastable defects, whose electronic properties are studied here. We also show that these metastable defects are not related to oxygen impurity concentration, and more importantly, they do not affect TR's beneficial suppression of oxygen precipitation because of TID during the solar cell process. Moreover, we show that external impurity gettering is further facilitated by the TR treatment.

2 | EXPERIMENTAL

The TR anneals are performed in a conventional hot-wall tube furnace at 1100°C for 10 minutes. The tube furnace has either a N_2, O_2, or a mixture of N_2 and O_2 as a gas ambient with a constant flow set at approx. 3.0 L/minute. The furnace is a Tempress model 203-6, and the loading and unloading of the wafers into and from the hot zone are done manually with a quartz push rod.

The wafers selected for these experiments are all *n*-type Cz, phosphorus-doped specified at 2 to 4 Ω cm, and <100> orientation. 156 mm pseudosquares are cleaved into individual pieces (quarters) approximately 60 mm × 60 mm and received Piranha and a full RCA clean. By subjecting individual quarters from the same wafer to different treatments and processing, we are able to avoid wafer-to-wafer and ingot-to-ingot variations. The wafers in Figures 1 and 4 are high-lifetime PV-grade wafers with O_i concentration of ~15 ppma (7.5×10^{17} cm^{-3}). Three individual quarter wafers receive a TR-pretreatment with pure N_2, 1:1 N_2/O_2, or a pure O_2 gas ambient, respectively. The fourth quarter wafer (no-TR samples in Figures 2 and 5) is held back from any TR pretreatment for evaluation of the original wafer's as-received lifetime and implied open-circuit voltage (iV_{OC}).

Subsequent to each of the TR pretreatments, the wafer quarters are processed with a thermal budget matching the 2-step process of

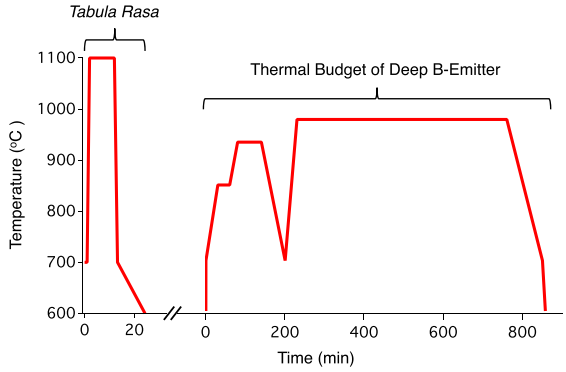

FIGURE 1 Thermal processing sequence profile that wafers are subjected to: TR high-T pretreatment (left) and thermal process identical to B-emitter formation and deep drive-in [Colour figure can be viewed at wileyonlinelibrary.com]

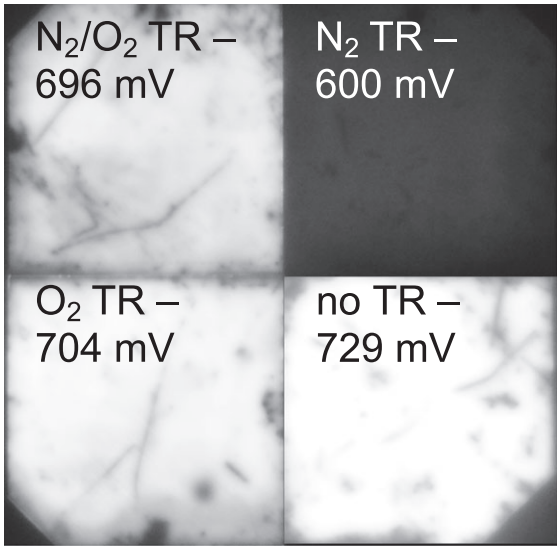

FIGURE 2 PL images of 3 n-Cz wafer quarters immediately after TR and 1 witness quarter without TR. TR in N_2/O_2 1:1 mixture; TR in N_2; TR in O_2; no TR. iV_{OC} values measured with a Sinton Instruments WCT-120 are noted in the figure

a deep diffused boron emitter similar to that of TOPCon cell on *n*-FZ by Richter et al.[2] The summary thermal process sequence for the wafers (including TR treatment) is shown in Figure 1.

Our process thermally mimics the deep B emitter process sequence and is performed in an inert N_2 ambient and in 1-continuous step, without any BBr_3 flow. As shown in Section 3, this thermal treatment induces TID because of the growth of OPN into highly recombination-active oxygen precipitates, without an additional impurity gettering effect by B. In our experiment, the impurities are separately post-gettered by $POCl_3$ process described below.

After each of the wafer sections are subjected to the B thermal budget, their surfaces are prepared with a full RCA cleaning procedure, and then passivated with ~15 nm of Al_2O_3 via atomic layer deposition by a Beneq TFS-200 system. This ALD process used TMA and H_2O as the process gases, and deposition is performed at 200°C, and with gas pulses of 300 milliseconds. Following the film deposition of Al_2O_3, we anneal all the wafers at 400°C in 10% H_2/90% N_2 forming gas to activate the atomic hydrogen and chemically passivate the surfaces of each wafer. Once passivated, the wafers are then measured and analyzed with a Sinton WCT-120 to establish implied open-circuit voltage (iV_{OC}) and also minority carrier bulk lifetime (τ_{bulk}). The iV_{OC} value is determined at absorbed photon flux equivalent to 1 sun, and the lifetime is determined as "high injection bulk lifetime" from the intercept of the inverse photocarrier lifetime-injection level curve. Temperature-dependent lifetime spectroscopy is performed on the same WCT-120 instrument equipped with a temperature-controlled stage. Photoluminescence (PL) imaging is also performed to reveal spatial information of the material quality.

To explore the effect of oxygen content (Figure 6) on the TID, we compare *n*-Cz wafers from 2 ingots with [O_i] concentrations of 11.8 and 15.9 ppma, while their as-received resistivity and thickness are similar (2-4 Ω cm, 170-180 μm). These wafers were chemically cleaned, TR-treated, and thermally postprocessed in the same way as the wafers in Figures 2 and 5. The whole treatment ends with the

thermal budget of a deep B drive-in and iV_{OC}, τ_{bulk}, and PL measurements. Following that, the 2 wafers with different $[O_i]$ have their Al_2O_3 layers stripped in dilute HF and then subjected to a phosphorus gettering process with a bubbled $POCl_3$ source. This gettering was performed in a separate hot-wall tube furnace at 650°C for 120 minutes. Once gettered, these wafer quarters are etched in 25% KOH to remove the top 5 μm of heavily P-doped material, then receive an RCA cleaning, and the new surfaces are passivated with Al_2O_3 followed by a forming gas anneal activation. iV_{OC} and τ_{bulk} are again measured with WCT-120, and PL is imaged.

3 | RESULTS

3.1 | Photocarrier lifetime change immediately after Tabula Rasa

The photoluminescence images of the *n*-Cz material immediately after TR are shown in Figure 2. We see that the TR annealing process decreases photocarrier lifetime in *n*-Cz wafers as evidenced by darkening of the PL and drop in the measured iV_{OC}. Specifically, the sample subjected to a N_2 TR pretreatment severely degrades, resulting in a 129 mV decrease of iV_{OC} from its as-received state of 729 mV.

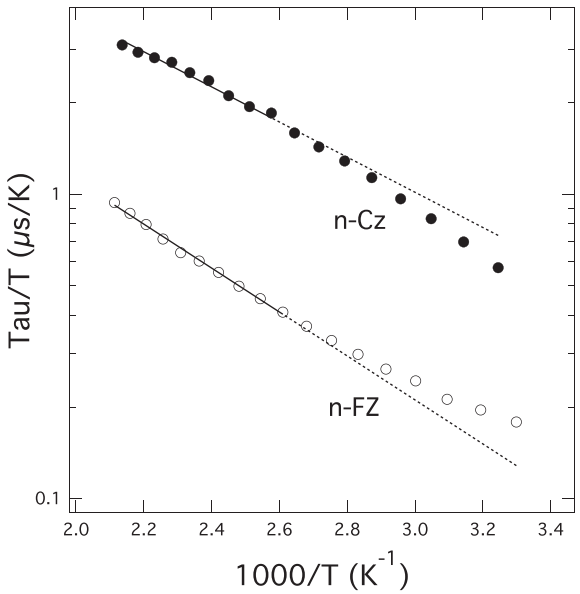

FIGURE 3 TDLS plot of *n*-type Si wafer samples after TR in N_2. Solid black circles: *n*-Cz sample subjected to N_2 TR of Figure 1. Open black circles: *n*-FZ wafer after the same N_2 TR. Solid portions of the lines are linear fits within 110 to 200°C range

Next, we investigate the mechanism behind the lifetime degradation in the N_2-treated material. We use the temperature-dependent lifetime spectroscopy (TDLS)[8] to identify the dominant defect responsible for this behavior. Figure 3 is an Arrhenius plot of the minority carrier lifetime to temperature ratio at a low injection level of approximately 10^{14} cm^{-3}. In addition to a *n*-Cz sample annealed with the identical conditions as the "N_2 TR" sample of Figure 1, the technique was also applied to a *n*-FZ material witness, resulting in similar degradation as seen in Figure 3, left. These FZ results resemble those of Grant et al[9] in nitrogen-doped FZ wafers with the important difference of processing in an inert environment in our case. The linear portion of the plot[8] for the *n*-Cz sample corresponds to a shallow defect with an energy level of 0.11 ± 0.03 eV. Similarly, a shallow defect level of 0.14 ± 0.03 eV is observed in the *n*-FZ material as well. These energy levels can be close to either conduction or valence band edges, because TDLS is not selective to the particular band edge.

These observations suggest that the defects responsible are unlikely to be associated with deeper metallic impurities.[10] Rather, intrinsic defects such as interstitials, vacancies, and their complexes appear as viable candidates. In addition, very similar defect properties in *n*-Cz and *n*-FZ samples suggest that the defect in question is not related to oxygen that is prevalent in Cz-Si.

Intrinsic point defects are known to be metastable at elevated temperatures.[8] To test this, and to exclude energetically-shallow metallic impurities, we subject the *n*-FZ samples identically processed to the N_2 TR sample of Figure 2 to an 850°C/30-minute annealing in forming gas. Indeed, the degraded lifetime rebounds, as shown in Figure 4 by considerably brighter PL after the FGA.

Because no gettering agent such as phosphorus was involved, this further confirms that the defects are intrinsic and metastable rather than metallic impurities. These will likely be eliminated because of thermal budget of cell processing, leading to final high lifetime cell wafer.

3.2 | Photocarrier lifetime improvement after Tabula Rasa and thermal budget of B-diffused cell process

Next, we subject the samples from Figure 2 to the B-emitter formation thermal budget, the most challenging part of the diffused *n*-type cell process, because of O precipitation. Figure 5 shows the PL images

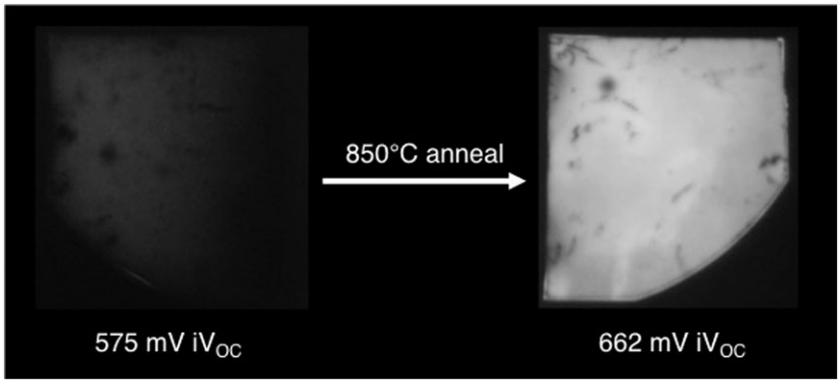

FIGURE 4 PL images of *n*-FZ samples processed identically to N_2 TR sample of Figure 1. Left: Immediately after N_2 TR. Right: After forming gas anneal at 850°C for 30 minutes subsequent to N_2 TR

of samples with various TR pretreatments (or no TR) after the B diffusion and deep drive-in thermal budget (see Section 2).

Notably, the iV_{OC} of the N_2 TR-treated sample has increased significantly after the B process from the state shown in Figure 2 whereas the no TR sample degrades down to 628 mV, making it unsuitable for high efficiency device manufacturing. The PL of the no TR sample reveals recombination-active regions forming a ring-like pattern. This is characteristic of O precipitation into P and L bands by O_i and multivacancies (nanovoids).[11] In TR-treated samples, the ring pattern is barely discernible, and the iV_{OC} is considerably higher. These results are particularly similar to the observations of Basnet et al in their study of TR on UMG Si.[6] Slight differences in iV_{OC} (barely beyond the measurement error of ~2 mV), however, are seen in the samples that underwent any TR pretreatment. Vacancy-injecting N_2 treatment appears somewhat less effective because of possible residual void formation by vacancy agglomeration.[11,12] In contrast, interstitial-injecting O_2 treatment leads to the highest iV_{OC} after the cell process.

We now explore the effect of TR on *n*-Cz wafers of 2 distinctly different interstitial oxygen concentrations: (1) the "low O_i" wafer at 11.8 ppma and (2) "high O_i" wafer at 15.9 ppma. It is worth noting that our low O_i wafers are exceptionally low in oxygen, approaching the practical lower limit of O_i in Si during the Cz crystal growth. Both wafers were quartered and subjected to various TR treatments slightly differed from those in Figure 2: no TR; TR in N_2; TR in O_2; TR in O_2 with extended cool down time of 90 minutes ("EX TR" in Figure 6). After that, all the samples underwent thermal process equivalent to the B diffusion and deep drive-in (without an actual in-diffusion of boron).

Table 1 shows the concentrations of interstitial oxygen [O_i] and substitutional carbon [C_s], measured in as-received state.

Notably, the low O_i wafers show significantly higher [C_s] than the high O_i wafers. Another important difference is thermal donor activity in as-received high O_i wafers. This is evidenced by ~3× wafer resistivity increase after TR treatment, which eliminates the thermal donors. Lengthy anneals near 450°C are known to create thermal donors,[13] which likely resemble the thermal history of our *n*-Cz ingots. In contrast, the thermal donor contribution to active dopants in low O_i wafer is small, likely because of its low oxygen content that sensitively affects thermal donor creation rate especially near 500°C.[13] The measured lifetime and iV_{OC} values discussed below take into account the wafer resistivity changes because of thermal donors.

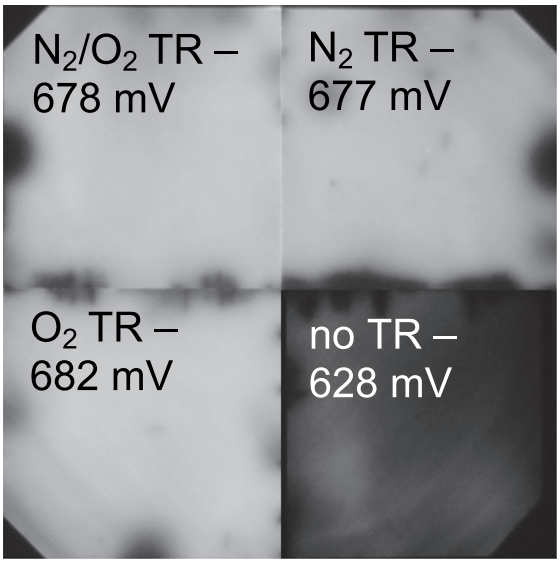

FIGURE 5 Photoluminescence images of *n*-Cz wafer quarters of Figure 1 after the thermal budget of B diffusion and deep drive-in. The "no-TR" quarter is from a nominally identical wafer that was not treated with TR before the B diffusion and deep drive-in thermal budget

TABLE 1 Interstitial oxygen [O_i] and substitutional carbon [C_s] concentrations in "high O_i" and "low O_i" wafers, along with wafer resistivity values before and after the *Tabula Rasa* treatment

n-Cz Wafer	[O_i] (ppma)	[C_s] (ppma)	R_{before} (Ω cm)	R_{after} (Ω cm)
High O_i	15.9	0.13	2.91	8.6
Low O_i	11.8	1.10	1.74	1.8

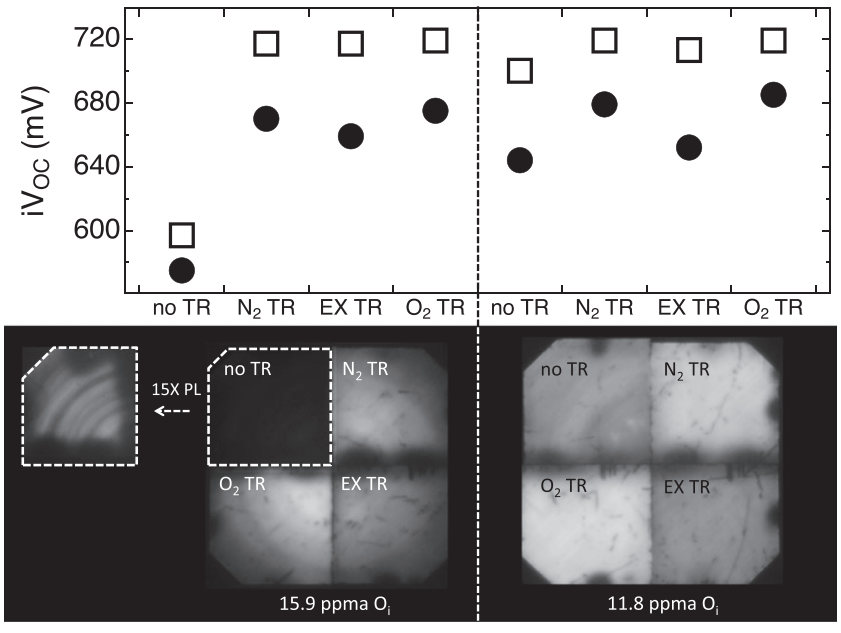

FIGURE 6 Top: Plot of iV_{OC} values after emitter thermal budget (black closed-circle symbols) and after subsequent phosphorus gettering (open-square symbols) in "high-O_i"/15.9 ppma (left) and "low-O_i"/11.8 ppma (right) samples. The *x*-axis table categorically denotes the different TR treatments before processing. Bottom: PL images of high O_i (left) and low O_i (right) wafers taken after different TR treatments as noted, followed by a thermal treatment equivalent to boron diffusion and deep dopant emitter drive-in. The inlayed PL image of non-TR-treated high O_i sample taken with an extended (15X) exposure reveals the characteristic recombination-active "swirl pattern"

Figure 6 shows the iV_{OC} after TR + boron emitter thermal budget (black closed-circle symbols). Consistent with the results from Figures 2–5, we observe pronounced improvement in iV_{OC} in the cases when TR was applied to the wafers prior to the aggressive thermal budget. The effect is most pronounced in the high O_i case, which is consistent with higher oxygen content that critically influences the O precipitate formation.[4]

The PL images in Figure 6 show the effect of TR treatment in both wafers. Without TR treatment, the high O_i wafer degrades significantly more than the low O_i wafer. Whereas, with TR treatment, the resulting iV_{OC} values are at least 670 mV, shown also in Figure 6 by black closed-circle symbols. The no-TR sample of the high O_i wafer exhibits recombination-active centers forming a characteristic swirl pattern, similar to the no-TR sample of Figure 6. The results of Figure 6 confirm that TR suppresses the oxygen-related TID by the cell processing sequence, especially in wafers with higher oxygen content.

Finally, we explore the efficacy of external gettering in wafers with TR, which can be impeded by the oxygen precipitates. For example, Zhang et al report an effective binding energy of 0.80 eV[14] between oxide precipitates and the gettered Fe impurities. Murphy et al have shown that these Fe-decorated precipitates have very high recombination activity, with large associated capture cross sections for both electrons and holes.[5] By eliminating precipitates, we expect the external gettering to improve, resulting in enhanced photocarrier lifetime.

When phosphorus gettering is applied (open symbols in Figure 6), we observe a significant increase in iV_{OC} and bulk lifetime in all TR-treated samples, resulting in iV_{OC} as high as 719 mV and bulk lifetime as high as 2.25 milliseconds. The material is almost revived to its as-received state (725 and 729 mV for high O_i and low O_i wafers, respectively). This observation is consistent with lower external gettering of Fe_i in the presence of O precipitates. In contrast, the no-TR, O-precipitated high-O_i witness sample still shows an iV_{OC} < 600 mV and bulk lifetime of ~200 microseconds after external gettering. Whereas, the no-TR, low-O_i witness sample is more responsive to gettering, yet the resulting iV_{OC} of 700 mV is still 19 mV less than both N_2 and O_2 TR samples of the same wafer.

Figure 7 shows lifetime injection level curves in high-O_i and low O_i after the external gettering, with lifetime injection level data points marked for the implied open-circuit voltage condition iV_{OC} (squares) and implied maximum power point condition iV_{MPP} (circles).

As seen from Figure 7, the highest lifetime at implied maximum power point condition is achieved in the high O_i wafer with *TR* pretreatment (above 2 milliseconds). The flatness of the lifetime injection level curve at lower injection levels indicates no significant deep Shockley-Read-Hall recombination center that would detrimentally affect cell performance at injection levels near or below the maximum power point. In contrast, the high O_i wafer shows a slight decline of the lifetime at lower injection as well as lower lifetime at the implied maximum power point.

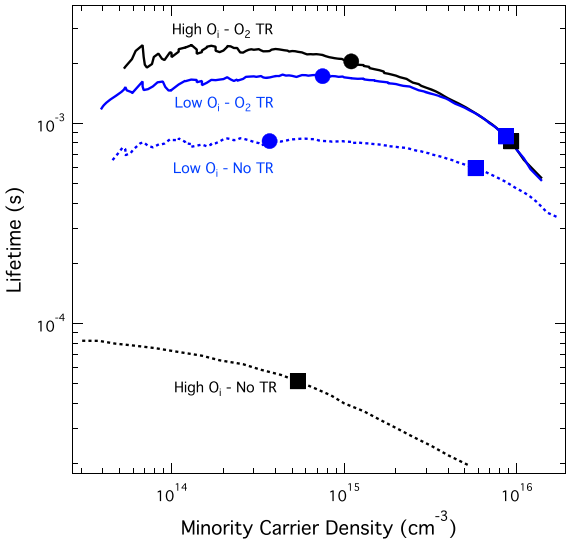

FIGURE 7 Injection-dependent lifetime spectra of *n*-Cz material measured with Sinton PCD. *Tabula Rasa* (or absence of), conditions are marked on the graph. Solid square markers on the curves represent the lifetime at 1-sun iV_{OC}, and the solid circle markers represent lifetime at V_{MPP}. Because of the extremely low lifetimes observed in the "high O_i-no TR" sample, the PCD analysis was unable to calculate a valid lifetime at V_{MPP} [Colour figure can be viewed at wileyonlinelibrary.com]

4 | DISCUSSION

In Figures 2–4, we observe strong variations in bulk carrier lifetime after TR when performed in different ambients: a relatively small reduction in lifetime for O_2 and very significant one for N_2 ambient. It might appear that TR treatment in inert N_2 is unsuccessful or even detrimental to cell performance. However, we further show that this is not the case and that TR ultimately improves the carrier bulk lifetime irrespective of the ambient it was performed (oxidizing or inert); see Figures 5 and 6. Below, we explain these observations based on the intrinsic and nature of these defects, a metastable by-product of TR.

Firstly, these lifetime-reducing defects because of N_2 ambient are metastable: They anneal out at 850°C for 30 minutes in an inert ambient (Figure 4). Secondly, the same bulk lifetime degradation is observed in FZ-Si (Figure 3), indicating that this phenomenon is not related to oxygen impurity. Likewise, the effect does not appear to be linked to any trace impurity. These observations suggest that the metastable carrier lifetime degradation is related to intrinsic defects: vacancies, interstitials, and their aggregates.

At the TR temperature of 1100°C, interstitials and vacancies (1) are continuously generated in the bulk as Frenkel pairs, (2) recombine in the bulk reforming Si lattice sites, (3) recombine (more precisely, annihilate) at the wafer surfaces, (4) diffuse, and (5) can be injected from the surfaces into the bulk because of a chemical reaction (such as oxidation) with an ambient. In addition, these defects can agglomerate and form complexes with impurities. Below, we outline how these processes may explain our results.

In a simplified picture (neglecting defect agglomeration, formation of complexes, etc.), interstitial and vacancy concentrations C_I and C_V are governed by 2 coupled differential equations[15] (presented as 1 indexed equation):

$$\frac{\partial C_{I,V}}{\partial t} = \nabla\cdot\left(D_{I,V}\nabla C_{I,V}\right) - K_R\left(C_I C_V - C_I^* C_V^*\right) \quad (1)$$

Here, D_I and D_V are diffusivities of interstitials or vacancies, respectively, and C_I^* and C_V^* are their equilibrium bulk concentrations. The corresponding bimolecular recombination rate $K_R C_I^* C_V^*$[16] is equal to the Frenkel pair generation rate at bulk equilibrium. Furthermore, the wafer surfaces introduce boundary conditions (here again represented by a single indexed equation), that balance the surface injection, surface recombination, and diffusive fluxes of the respective species (*I* or *V*):

$$g_{I,V} = D_{I,V} \nabla C_{I,V} \cdot \vec{n} + K_{surf\ I,\ V} \quad (2)$$

Here, g_I and g_V are surface injection fluxes for the interstitials and vacancies and $K_{surf\ I,\ V}$ are their respective surface recombination (annihilation) fluxes governed by recombination velocities.

Figure 2 shows that TR performed at 1100°C in O_2 degrades the minority carrier lifetime in the *n*-Cz wafer significantly less than TR performed in an N_2 ambient. Because the wafer surface is being oxidized during the TR in O_2, additional self-interstitials are injected into the bulk[17] from the surface source.[15,18] This results in factor 4-5 enhancement C_I/C_I^* of interstitial concentration within 10 minutes of oxidation at 1100°C,[15] without reaching a steady-state condition[19] in Equation (1). The diffusivities of both vacancies and interstitials are sufficiently high at the temperature of the TR. Even assuming the low estimate of $D_{I,V} > 10^{-6}$ cm^2/second over the range of measured literature values,[16,20], both vacancies and self-interstitials diffuse through the whole ~200-μm wafer thickness during TR at 1100°C for 10 minutes and establish approximately uniform bulk concentrations. Increased bulk interstitial concentration C_I reduces that of vacancies C_V via reducing vacancy bulk recombination lifetime $1/K_R C_I$; see Equation (1). In this process, the product $C_I C_V$ remains close, but not equal to the equilibrium product $C_I^* C_V^*$ because due to the surface injection and recombination (more precisely annihilation), not all *I* and *V* are created, or annihilate, as pairs.[15,19] Thus, our TR treatments in O_2 produce a vacancy-suppressed wafer bulk.

In contrast, when TR is performed in N_2, no interstitial injection is expected. Under this condition, we find considerable minority carrier lifetime degradation immediately after the TR treatment. We performed XPS studies on our N_2 TR-treated wafers and have found N signal at close to the noise level, indicating negligible nitridation. We also performed TR in Ar gas environment on a wafer identical to that of Figure 1. The after-TR iV_{OC} = 600 mV, the same low value as for TR in N_2 (Figure 2), therefore, inert gas environment during TR being a key to increased carrier recombination activity in the wafer.

With wafer in inert ambient, we can consider *I* and *V* being generated thermally mostly in the bulk, reaching wafer surfaces by diffusion and annihilating at the wafer surfaces. The literature values vary over wide range, some studies suggesting faster diffusion of interstitials: D_I ~10^{-4} cm^2/second near[16] and D_v ~10^{-5} cm^2/second at 1100°C.[21] Faster diffusion of interstitials facilitates their surface annihilation and lowering of their bulk concentration C_I. This, in turn, leads to the reduction of bulk recombination of vacancies (via the term $K_R C_I C_V$ in Equation (1)) and their higher steady-state concentrations. A fraction of steady-state vacancy concentration is preserved during the rapid cool down following the *TR* treatment. Therefore, we suggest that TR treatments in N_2 produce vacancy-rich wafer bulk that enhances minority carrier recombination.

Indeed, our shallow defect level measured by TDLS from Figure 3 is consistent with vacancy-associated hole traps separated from the valence band of Si by 0.11 to 0.14 eV measured by DLTS.[16] This carrier lifetime degradation occurs both in *n*-FZ and in *n*-Cz wafers; thus, it is not related to oxygen impurities.

The metastable nature of this defect (see Figure 4, annealing out at 850°C) further supports our vacancy hypothesis for degradation after TR in N_2. At 850°C, the intrinsic defect generation in the bulk is negligibly low, because of the high activation energy for the Frenkel pair generation (>5 eV for *n*-type Si[22]). On the other hand, even with low estimate for vacancy diffusion D_V ~10^{-8} cm^2/second at this temperature,[20] their diffusion length during 30 minutes at 850°C is about 40 μm, comparable to half-wafer thickness. Therefore, most of the metastable vacancies are able to reach the wafer surface and annihilate there, if the bulk recombination is suppressed because of low C_I. In the absence of surface injection, this leads to the annealing of previously created metastable vacancy and interstitial populations, consistent with negligibly small bimolecular bulk equilibrium recombination rate $K_R C_I^* C_V^*$[16] at this temperature.

As shown in Figures 5–7, TR has strong beneficial effects on bulk wafer quality (minority carrier lifetime) after the cell processing steps that would normally lead to oxygen precipitation and lifetime degradation. *Tabula Rasa* performed in different ambient conditions might modify the frozen-in vacancy or interstitial concentrations C_I and C_V as discussed above, but this is a metastable effect and gets "erased" as it is annealed out during the cell process at elevated temperatures ~850°C. Therefore, the main effect of TR—dissolution of OPN—is independent of the TR ambient (O_2, N_2). Figures 5–7 show high final iV_{OC} and minority carrier lifetime values in all TR-treated wafers through the subsequent high thermal budget of boron diffusion. The dissolution of OPN thus appears to be the critical result of the TR independent of the ambient. As additional conclusion, performing cell processes in oxidizing ambient is expected to suppress the O precipitation because of the injection of interstitials to lower concentrations of vacancies that promote O precipitate growth.[12]

The oxygen content in *n*-Cz wafers significantly affects O precipitation,[4] as demonstrated in Figure 6. However, even the low O_i Cz wafer still benefits from a TR treatment before the high-temperature cell processing budget that simulates deep B drive-in. Surprisingly, TR-treated high O_i wafers show higher lifetimes at implied maximum power point carrier injection level than the low O_i wafers. This difference might be attributed to ~8× higher substitutional carbon content in low O_i wafers. At the same time, this higher carbon content is still below the approximate threshold of 2 ppma of carbon-enhanced O precipitation.[23]

We note the similarity of the results obtained after an actual B diffusion and deep drive-in, to an identical thermal treatment without in-diffusing boron used in this work. Both approaches confirm that the thermal-induced degradation is caused from oxygen precipitation[5] and not the boron diffusion itself. Rather, actual B diffusion likely improves the final lifetime by external gettering and possibly through the interstitial-injecting oxidation as part of B drive-in. Indeed, we have demonstrated in our previous work[24] a symmetric, passivated B emitter on TR-treated *n*-Cz wafer with iV_{OC} = 717 mV. A solar cell structure with passivated, deep B emitter at the front and n+poly-Si/

tunneling SiO_2 passivated back-surface field contact on the back, exhibiting iV_{OC} = 724 mV before metallization.[24] This excellent cell performance is principally enabled by the TR pretreatment, because without it, the resulting iV_{OC} in both devices was <650 mV because of the cell process-degraded bulk. In addition to the above, we have achieved iV_{OC} = 735 mV on a symmetric, P-doped poly-Si/SiO_2 passivated BSF contact to the *n*-Cz wafer, where the wafer has been TR-treated prior to passivated contact fabrication.[24] The high iV_{OC} value confirms that excellent cell performance can be obtained in TR-pretreated wafers, provided that some external gettering mechanism (B and P diffusions, poly-Si) is in place.

Our *Tabula Rasa* treatments are performed in a conventional diffusion furnace, therefore can be implemented on industrial scale to improve the Cz-Si wafer-based cell efficiency and process yield. For example, wafers from the ends of ingots with higher [O_i] and vacancy concentrations will exhibit less lifetime degradation during high-temperature thermal histories, so that a larger portion of the ingot can be used provided that the "marginal" wafers get *Tabula Rasa* treatment.

5 | CONCLUSIONS

We have shown that *Tabula Rasa* performed in any of the gas-environments studied makes *n*-Cz wafers significantly more resistant against cell process-induced degradation[3] and more responsive to impurity gettering. *Tabula Rasa* appears to be accompanied by creation of metastable vacancies when performed in inert (N_2) gas ambient. These defects significantly reduce the minority carrier lifetime. An oxidizing (O_2) gas ambient during TR significantly suppresses these metastable vacancies, by offsetting the thermal equilibrium concentration of vacancies with oxidation-injected interstitials.[25] Most importantly for solar cell process, these metastable defects anneal out at typical cell processing temperatures ~850°C, revealing the essential effect of TR: dissolving OPN. This dissolution of OPN ultimately leads to enhanced photovoltaic performance with TR-treated *n*-Cz wafers. The beneficial effect of *Tabula Rasa* treatment is particularly pronounced in *n*-Cz wafers with high interstitial oxygen content that are more prone to oxygen precipitation.

ACKNOWLEDGEMENTS

The authors thank Hao-Chih Yuan, Bhushan Sopori, Harold Korb, and Greg Wilson for useful discussions and Steven Johnston for help with photoluminescence experiments, and Craig Perkins for XPS measurements.

This work was authored in part by the National Renewable Energy Laboratory, operated by Alliance for Sustainable Energy, LLC, for the US Department of Energy (DOE) under Contract No. DE-AC36-08GO28308. Funding was provided by US Department of Energy Office of Energy Efficiency and Renewable Energy Solar Energy Technologies Office under contract DE-EE00030301. The views expressed in the article do not necessarily represent the views of the DOE or the US Government. The US Government retains and the publisher, by accepting the article for publication, acknowledges that the US Government retains a nonexclusive, paid-up, irrevocable, worldwide license to publish or reproduce the published form of this work, or allow others to do so, for US Government purposes.

M. A. Jensen and E. E. Looney acknowledge support by the National Science Foundation Graduate Research Fellowship under Grant 1122374.

ORCID

Vincenzo LaSalvia http://orcid.org/0000-0003-1437-4153

REFERENCES

1. Pagani M, Falster RJ, Fisher GR, Ferrero GC, Olmo M. Spatial variations in oxygen precipitation in silicon after high temperature rapid thermal annealing. *Appl Phys Lett*. Mar. 1997;70(12):1572-1574.
2. Richter A, Benick J, Feldmann F, Fell A, Hermle M, Glunz SW. N-type Si solar cells with passivating electron contact_ identifying sources for efficiency limitations by wafer thickness and resistivity variation. *Sol Energy Mater Sol Cells*. Dec. 2017;173:96-105.
3. Walter DC, Lim B, Falster R, Binns J, Schmidt J. Understanding lifetime degradation in Czochralski-grown N-type silicon after high-temperature processing. Proc. 28th Eur. Photovoltaic Sol. ..., 2013.
4. Falster R, Cornara M, Gambaro D, Olmo M, Pagani M. Effect of high temperature pre-anneal on oxygen precipitates nucleation kinetics in Si. *SSP*. 1997;57:123-128.
5. Murphy JD, McGuire RE, Bothe K, Voronkov VV, Falster RJ. Minority carrier lifetime in silicon photovoltaics—the effect of oxygen precipitation. *Sol Energy Mater Sol Cells*. Jan. 2014;120, no. PA:402-411.
6. Basnet R, Rougieux FE, Sun C, et al. Methods to improve bulk lifetime in n-type czochralski-grown upgraded metallurgical-grade silicon wafers. *IEEE J Photovoltaics*. Jul. 2018;8(4):990-996.
7. Kelton KF, Falster R, Gambaro D, Olmo M, Cornara M, Wei PF. Oxygen precipitation in silicon: Experimental studies and theoretical investigations within the classical theory of nucleation. *J Appl Phys*. Jun. 1999;85(12):8097-8111.
8. Rein S, Rehrl T, Warta W, Glunz SW. Lifetime spectroscopy for defect characterization: systematic analysis of the possibilities and restrictions. *J Appl Phys*. Feb. 2002;91(4):2059-2070.
9. Grant NE, Markevich VP, Mullins J, et al. Permanent annihilation of thermally activated defects which limit the lifetime of float-zone silicon. *Physica Status Solidi (a)*. May 2018;213(11):2844-2849.
10. Sze SM, Ng KK. *Physics of Semiconductor Devices*. Hoboken, NJ, USA: John Wiley & Sons, Inc.; 2006.
11. Falster R, Voronkov VV, Quast F. On the properties of the intrinsic point defects in silicon: a perspective from crystal growth and wafer processing. *Phys Stat Sol (b)*. Nov. 2000;222(1):219-244.
12. Falster RJ, Pagani M, Gambaro D, et al. Vacancy-assisted oxygen precipitation phenomena in Si. *SSP*. 1997;57:129-136. 57-58
13. Londos CA, Binns MJ, Brown AR, McQuaid SA, Newman RC. Effect of oxygen concentration on the kinetics of thermal donor formation in silicon at temperatures between 350 and 500 °C. *Appl Phys Lett*. Mar. 1993;62(13):1525-1526.
14. Zhang P, Istratov AA, Väinölä H, Weber ER. Re-dissolution of Gettered Iron impurities in Czochralski-grown silicon. *SSP*. 2004;95:577-580.
15. Law ME, Haddara YM, Jones KS. Effect of the silicon/oxide interface on interstitials: Di-interstitial recombination. *J Appl Phys*. Oct. 1998;84(7):3555-3560.
16. Pichler P. *Intrinsic Point Defects, Impurities, and Their Diffusion in Silicon*. Vienna: Springer Vienna; 2004:105-106 (vacancy energy level)– 114–120 (vacancy diffusion)– 141–147 (interstitial diffusion)– 165 (bulk recombination rate).
17. Rougieux FE, Nguyen HT, Macdonald DH, Mitchell B, Falster R. Growth of oxygen precipitates and dislocations in Czochralski silicon. *IEEE J Photovoltaics*. Mar. 2017;1-6.
18. Hu SM. Kinetics of interstitial supersaturation and enhanced diffusion in short-time/low-temperature oxidation of silicon. *J Appl Phys*. Dec. 1985;57(10):4527-4532.

19. Hu SM. Interstitial and vacancy concentrations in the presence of interstitial injection. *J Appl Phys*. Jun. 1998;57(4):1069-1075.
20. Voronkov VV, Falster R. The diffusivity of the vacancy in silicon is it fast or slow? *Mater Sci Semicond Process*. Dec. 2012;15(6):697-702.
21. Voronkov VV, Falster R. Vacancy-type microdefect formation in Czochralski silicon. *J Cryst Growth*. Nov. 1998;194(1):76-88.
22. Goedecker S, Deutsch T, Billard L. A Fourfold coordinated point defect in Silicon. *Phys Rev Lett*. May 2002;88(23):235501.
23. Sun Q, Yao KH, Lagowski J, Gatos HC. Effect of carbon on oxygen precipitation in silicon. *J Appl Phys*. May 1990;67(9):4313-4319.
24. W. Nemeth, V. LaSalvia, M. R. Page, E. L. Warren, A. Dameron, A. G. Norman, B. G. Lee, D. L. Young, and P. Stradins, "Implementation of tunneling pasivated contacts into industrially relevant n-Cz Si solar cells," Presented at the 2015 IEEE 42nd Photovoltaic Specialists Conference (PVSC), 2015;1–3.
25. Dunham ST. Interactions of silicon point defects with SiO2 films. *J Appl Phys*. Aug. 1998;71(2):685-696.

How to cite this article: LaSalvia V, Youssef A, Jensen MA, et al. *Tabula Rasa* for *n*-Cz silicon-based photovoltaics. *Prog Photovolt Res Appl*. 2018;1–8. https://doi.org/10.1002/pip.3068